



How to cite this article:

Authors: Piotr Połowniak, Mariusz Sobolak

Title of article: „Analiza śladu styku zębów w przekładni ślimakowej globoidalnej w środowisku CAD” (“Contact pattern analysis in globoidal worm gear performed in CAD environment”)

Mechanik, Vol. 91, No. 1 (2018): pages 70–72

DOI: <https://doi.org/10.17814/mechanik.2018.1.16>

Contact pattern analysis in globoidal worm gear performed in CAD environment

Analiza śladu styku zębów w przekładni ślimakowej globoidalnej w środowisku CAD

PIOTR POŁOWNIAK
MARIUSZ SOBOLAK *

Presented is the method of determining the contact pattern in globoidal worm gear using CAD environment. Contact pattern analysis was performed for the gear with straight tooth profile in the central plane. The influence of the pressure angle on the shape and size of the contact pattern was investigated.

KEYWORDS: globoid worm gear, contact pattern analysis

The contact trace is the surface on the side of the tooth where the surface of the second tooth cooperates at a given moment. There are several methods of obtaining a trace of tooth contact between gears [4, 5]. It can be differentiated the analytical or analytical and numerical method of solving the equations of meshing, the direct method in CAD environment can be used by designating a intersecting part of models (penetration equal to, for example, oil film thickness) or using FEM analysis (determination of thickness oil film).

The methodology of CAD modeling of the globoid worm and gear with a straight tooth profile in the central plane was described in [1–3]. The next step is to model several gear pairs and analyze the contact pattern with the direct CAD method.

Determination of the contact pattern by the direct CAD method

The CAD model of worm and worm wheel is put into a gear – as in fig. 1. The worm wheel model rotates by such an angle with respect to the x_2 axis so that it penetrates into the worm side to the given δ_w value measured in the central plane (fig. 2). Parameters have been introduced for the relative rotation of the worm φ_1 and worm wheel φ_2 and the penetration size of solids δ_w . By simulating the work of the transmission, the models rotate with established discrete step in accordance with the transmission ratio. At the given position of the gear elements, the common part of the worm and worm wheel model is determined.

The envelope formation forms and the contours are filled with the surface (Fill) (fig. 3). The surface areas of the contact pattern can be determined directly by measuring the surface of the flake elements or by analyzing the volume of the formed solids. Then it can be assumed that the ratio of

volume of solids to the surface area of their envelopes is approximately constant [4].

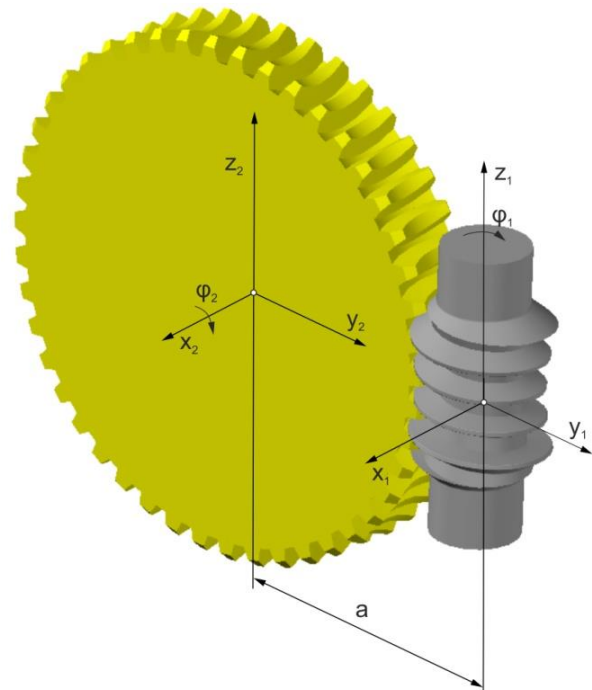


Fig. 1. Kinematic system of the globoidal worm gear (description in the text)

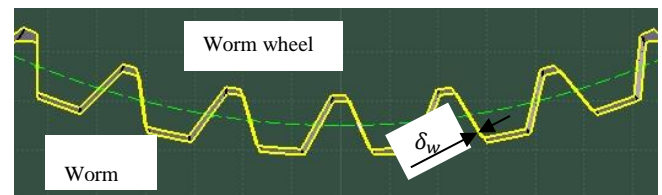


Fig. 2. Penetration of solids presented in the central plane of the gear

Fig. 3 shows an example of a temporary contact trace against the background of the worm wheel model.

Fig. 4 shows the determined values of the area of the contact pattern in a given part of the worm and the total contact region for the given gear set.

The surface area is determined using the Measure Item or Measure Inertia function. In both cases, the sizes of

* Dr inż. Piotr Połowniak (ppolowniak@prz.edu.pl), dr hab. inż. Mariusz Sobolak prof. PRz (msobolak@prz.edu.pl) – Katedra Konstrukcji Maszyn, Wydział Budowy Maszyn i Lotnictwa Politechniki Rzeszowskiej

surface areas in the structural tree are obtained, as well as in the graphical form, as in fig. 4. In the case of using the second method, it is possible to export the results directly to the txt file. A file is generated with the surface area of the given contact region as well as the total contact at the given gear set.

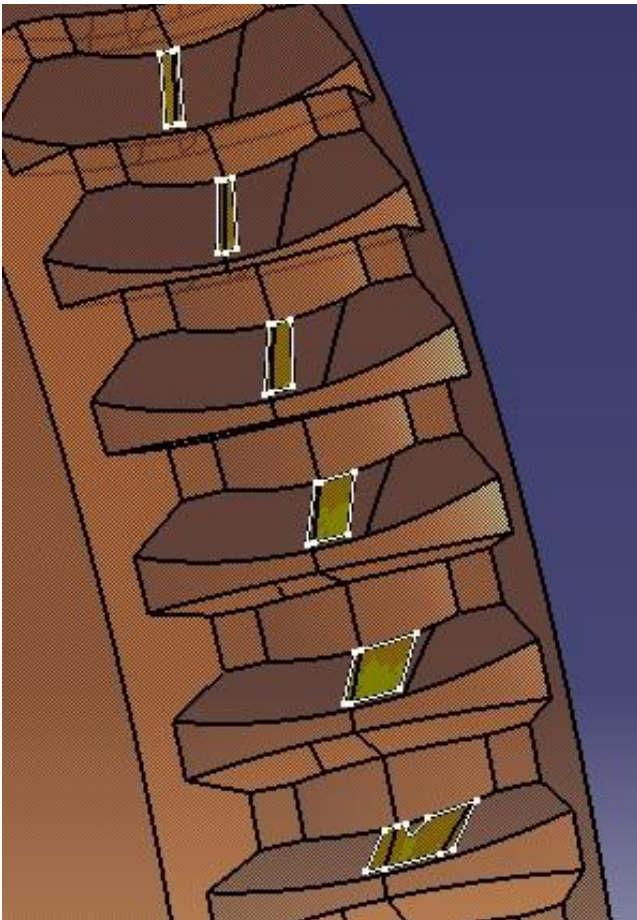


Fig. 3. Example of a temporary contact pattern shown on the worm wheel model

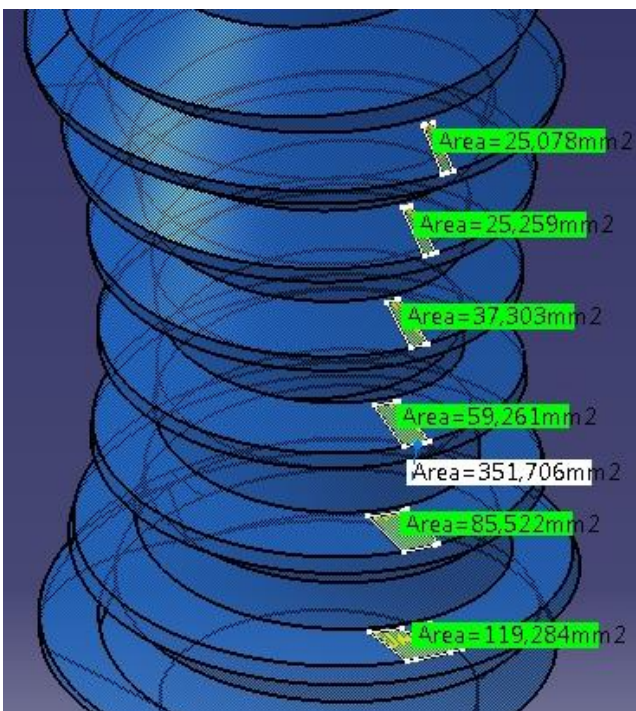


Fig. 4. Example of a temporary contact pattern shown on the worm model with the marked area of the contact region in a given part of the worm and the total field

Presented method of direct CAD determination of the contact pattern enables the analysis of the shape of the contact region and the creation of graphs, which present changes of the contact surface area depending on the rotation of the worm. Assuming that the surface areas of the contact region in a given gear position reflect their share in the load transfer, charts of the percentage of the contact region in the load transmission can be made.

Analysis of the results of the contact region using the direct CAD method

The table shows the geometric data of the gear on the basis of which the CAD models were made. In the case of a straight tooth profile, the pressure angle $\alpha_n = 20^\circ$ and $\alpha_n = 25^\circ$ was assumed.

Analyses of the contact region with the CAD method were made with the assumption that the body penetration in the central plane was 0.02 mm. Fig. 5 shows selected temporary regions of contact against the background of the worm model for two variants at a particular worm position.

The following figures (figs. 6–9) show the analysis of changes in the surface area of the contact pattern depending on the worm rotation and the share of these contact regions in the load transmission for the pressure angle $\alpha_n = 20^\circ$ and $\alpha_n = 25^\circ$. The horizontal axis of the diagrams is made without taking into account the scale, and the searching area for the field of contact region during the meshing of the beginning of the worm tooth is compacted.

Fig. 10 compares the total area of the contact region for $\alpha_n = 20^\circ$ and $\alpha_n = 25^\circ$.

From the analysis of the shape of the contact pattern at different pressure angles, it results that with the increase of the pressure angles, the first contact region is characterized by a greater degree of filling in the internal area. In the range of approx. 4° to 36° , the first contact region is larger for larger pressure angles. In other cases, the contact regions are similar in size, with a slight difference in favour of globoidal worm gear with smaller pressure angles. Therefore, in fig. 10 it can be seen that in the majority of the worm rotation cycle the total contact region is larger for the variant $\alpha_n = 20^\circ$ than for $\alpha_n = 25^\circ$. These observations are related to the shape of the side of the wheel tooth (fig. 11).

TABLE. Geometric data of the analyzed gears

	Worm	Worm wheel
Normal module, mm	$m_n = 7.1365$	
Number of worm teeth	$z_1 = 1$	$z_2 = 46$
Axis distance, mm	$a = 200$	
Pitch diameter, mm	$d_{w1} = 70$	$d_{w2} = 330$
Tip diameter, mm	$d_{a1} = 80.09$	$d_{a2} = 340.09$
Base diameter, mm	$d_{f1} = 57.7$	$d_{f2} = 317.67$
Effective length of the worm/Width of the worm wheel rim, mm	$b_{1eff} = 135$	$b_2 = 57$
Active range of the worm	$\varphi_{1p} = -5.8\pi$	$\varphi_{1k} = 5.8\pi$
Normal pressure angle, °	$\alpha_n = 20^\circ$ (variant I) $\alpha_n = 25^\circ$ (variant II)	

Fig. 11 shows the regions of the gear tooth side. Regions I and III are shaped by the extreme edge of the tool, while region II results from the envelope of the tool [2, 3]. In addition, the figure shows auxiliary vertical lines to show the difference in the widths of the middle region. For smaller pressure angles, the width of the region II of wheel is greater. Hence, the larger area of the contact patterns in the area of wheel region II, and also the larger surface area of

the first contact pattern for the pressure angle $\alpha_n = 25^\circ$ in the specified worm rotation range (about 4° to 36°).

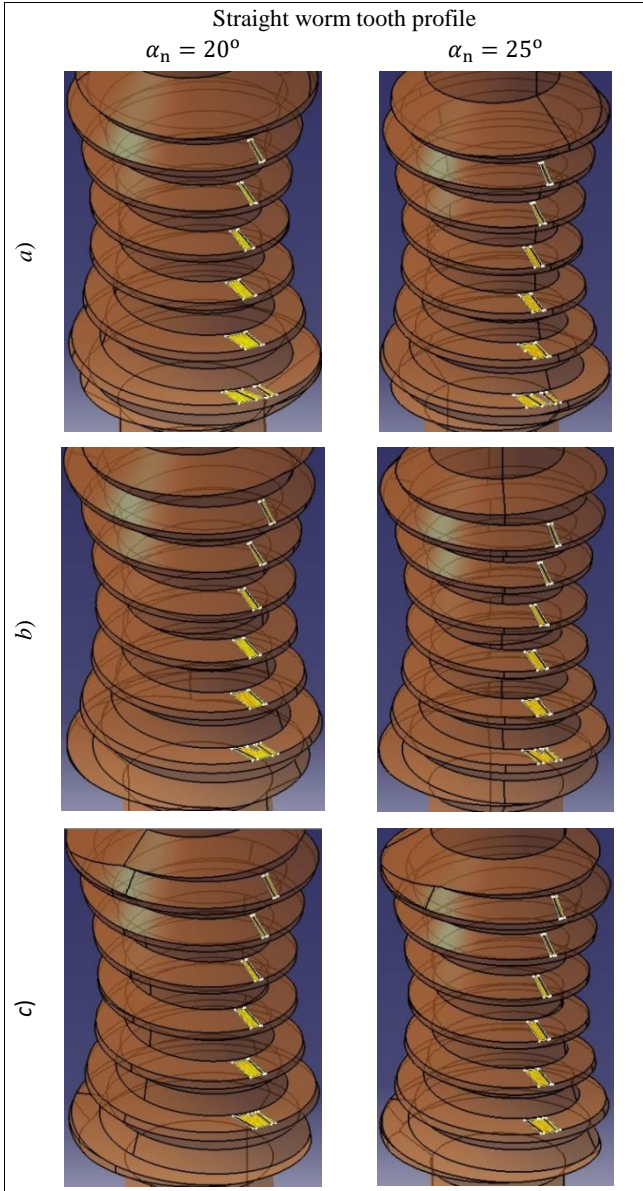


Fig. 5. The momentary contact pattern shown on the worm at the rotation angle: a) $\phi_1 = 0^\circ$, b) $\phi_1 = 144^\circ$, c) $\phi_1 = 216^\circ$

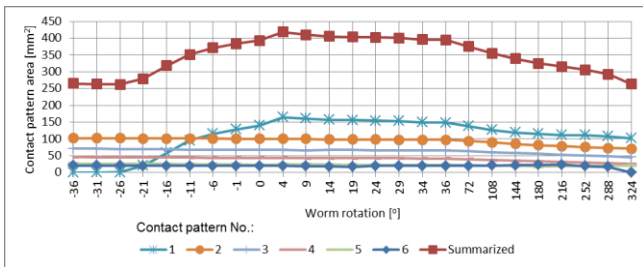


Fig. 6. Contact region area at $\alpha_n = 20^\circ$ (horizontal axis without scale)

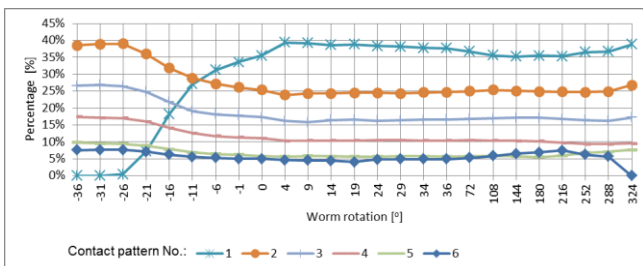


Fig. 7. Percentage of the contact pattern in the load transmission at $\alpha_n = 20^\circ$ (horizontal axis without scale)

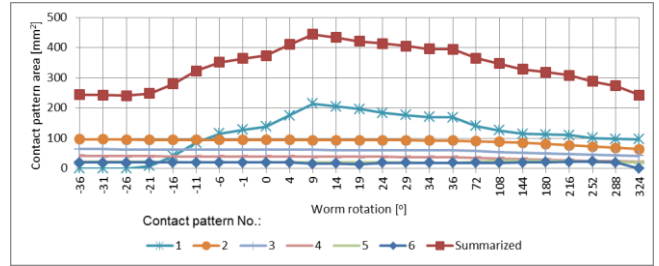


Fig. 8. Contact region area at $\alpha_n = 25^\circ$ (horizontal axis without scale)

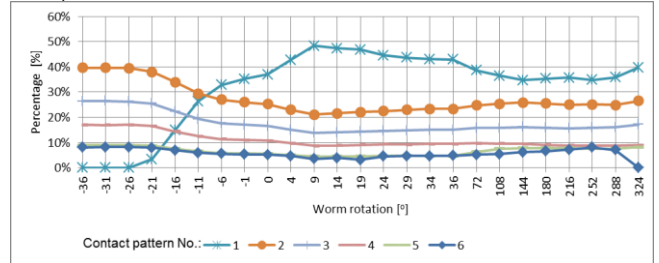


Fig. 9. Percentage of the contact pattern in the load transmission at $\alpha_n = 25^\circ$ (horizontal axis without scale)

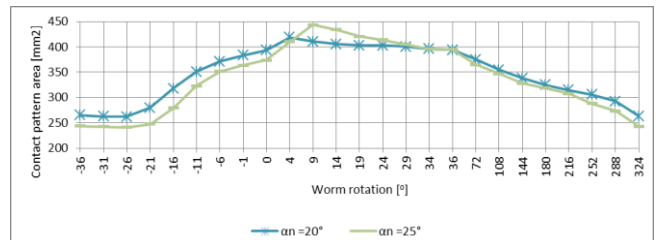


Fig. 10. Comparison of contact pattern area for $\alpha_n = 20^\circ$ and $\alpha_n = 25^\circ$ (horizontal axis without scale)

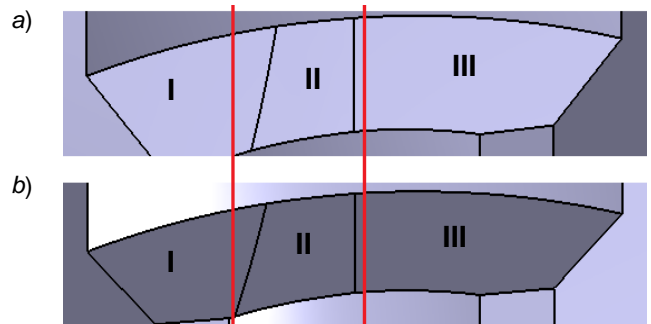


Fig. 11. Fragment of the gear side with separated regions: a) for $\alpha_n = 25^\circ$, b) for $\alpha_n = 20^\circ$

Conclusions

The following conclusions can be formulated on the basis of the contact pattern analysis in globoidal worm gear:

- At the entrance in mesh in the area of beginning of worm tooth, the participation of the first contact pattern in the load transmission grows rapidly. The unfavorable distribution of the first contact region is short-lived, within a few or more degrees of worm rotation. This condition can cause unfavorable fatigue stresses and chipping this piece of worm tooth. Therefore, it is advantageous to make a tooth end with a line modification. The stiffness of this part increases. The distribution of the contact pattern fields on the next part of tooth is even.
- The surface area of the first contact pattern during the cycle is the largest, and on each next part of the worm tooth (each next tooth of the wheel being in contact with the worm) the contact pattern is smaller. It can be concluded that the initial part of the worm tooth carries the largest loads.
- Depending on the position of the worm, the number of gear teeth being in simultaneous contact with the worm is 1.

In the worm positions in which a smaller number of gear teeth is in mesh, the total contact pattern area is the smallest (applies to the worm rotation range approx. 0.1π).

REFERENCES

1. Połowniak P., Sobolak M. „Modelowanie ślimaka globoidalnego w środowisku CAD”. *Mechanik*. 1 (2015): pp. 71–74.
2. Połowniak P., Sobolak M. „Modelowanie ślimaczniicy przekładni ślimakowej globoidalnej w środowisku CAD”. *Mechanik*. 3 (2015): pp. 250–252.
3. Połowniak P., Sobolak M. „Wpływ skrajnej krawędzi frezu ślimakowego na kształtowanie boku zęba ślimaczniicy”. *Mechanik*. 7 (2015): pp. 625–627.
4. Sobolak M. „Analiza i synteza współpracy powierzchni kół zębatych metodami dyskretnymi”. Oficyna Wydawnicza PRz, 2006.
5. Wiktor J. „Analityczno-numeryczne metody analizy parametrów geometrycznych, zakłóceń ruchu i wytrzymałości przekładni walcowych”. Oficyna Wydawnicza PRz, 2004.



Translation of scientific articles, their computer composition and publishing them on the website www.mechanik.media.pl by original articles in Polish is a task financed from the funds of the Ministry of Science and Higher Education designated for dissemination of science.



Ministry of Science
and Higher Education

Republic of Poland